

El Niño–Like Climate Teleconnections in New England During the Late Pleistocene

Tammy M. Rittenour,^{1*}† Julie Brigham-Grette,¹ Michael E. Mann²

A glacial varve chronology from New England spanning the 4000-year period from 17,500 to 13,500 calendar years before the present was analyzed for evidence of climate variability during the late Pleistocene. The chronology shows a distinct interannual (3 to 5 years) band of enhanced variability suggestive of El Niño–Southern Oscillation (ENSO) teleconnections into North America during the late Pleistocene, when the Laurentide ice sheet was near its maximum extent and climatic boundary conditions were different than those of today. This interannual variability largely disappears by the young end of the 4000-year chronology, with only the highest frequency components (roughly 3-year period) persisting. This record provides evidence of ENSO-like climate variability during near-peak glacial conditions.

The unusual recent behavior of ENSO, including the exceptionally strong warm events of 1982–83 and 1997–98 and the predominance of El Niño–like conditions during the past two decades (1), has highlighted the possibility that ENSO may be influenced by anthropogenic forcing (2). The limited success of models in predicting El Niño events (3) and the nonstationary statistical character of ENSO (4) and its teleconnections (5, 6) over the past two centuries indicate that our understanding of ENSO from the short instrumental record is incomplete. Thus, there is considerable interest in the long-term evolution of ENSO and its relation to low-frequency climate forcing.

Paleoclimate studies using tree rings, corals, and ice cores support the existence of century-scale irregularities in the character of ENSO variability (6, 7). For example, during the late 17th through mid-19th century, decadal ENSO-like variability persisted and interannual ENSO variability was strongly muted (6–8). The fact that this interval corresponds to a period of substantially lowered solar irradiance (the “Spörer Minimum”) has prompted speculation that solar forcing may influence the amplitude of interannual ENSO variability (6). Similarly, models suggest that greenhouse radiative forcing may lead to decreased amplitude of interannual ENSO variability (2).

Paleoclimate records show fluctuations in the intensity of ENSO variability during the Holocene. Coral isotopic data from the Great

Barrier Reef (9), a region currently influenced by ENSO, indicate warmer conditions with an absence of interannual variability during the middle Holocene, suggesting that ENSO (or its teleconnections to this region) was suppressed or absent at this time. Similar evidence for reduced ENSO variability during the middle Holocene was found in records from Australasia (10). Faunal records off the coast of Peru (11) have been used to suggest that ENSO events are a middle to late Holocene phenomena, but this interpretation is controversial (12). However, storm-induced debris flows at the low-frequency limit of the conventional ENSO band from a lake in Ecuador defy this interpretation and may extend the record of ENSO activity to 7000 calendar years before the present (cal yr B.P.) and possibly to 15,000 cal yr B.P. (13). In addition, spectral analysis of 264 glacial varves from the Lake Huron basin indicates the presence of ENSO-like interannual variability immediately after the Younger Dryas (~12,000 cal yr B.P.) (14). However, additional late Pleistocene records are needed to confirm the presence and nature of ENSO variability before the middle Holocene.

From a dynamical perspective, it is likely that astronomical forcing has modulated the amplitude and frequency of El Niño variability (15). Modeling results (16) suggest that precessional forcing should have sharply reduced the frequency of strong El Niño events before the middle Holocene, although interannual ENSO variability may not have ceased altogether. A recent modeling experiment forced by early Holocene insolation (15) shows a decreased amplitude of low-frequency variability but a persistence of high-frequency ENSO variability in relation to modern climate. It has not yet been possible to examine interannual ENSO-related variability over millennial-scale changes in

insolation and during late Pleistocene glacial conditions.

We analyzed the recently revised New England (NE) varve chronology based on varves from proglacial lakes formed during the recession of the Laurentide ice sheet 17,500 to 13,500 cal yr B.P. (Fig. 1). Thick clastic varves formed because of seasonal changes in sediment deposition (melt season versus lake ice cover), with the coarser melt-season layer contributing most of the variation in varve couplet thickness (17). Annual varve thickness was a function of glacial melting and surface runoff controlled by regional climate, allowing varves to be correlated within and between contemporaneous proglacial lakes throughout New England (18, 19). Ice-proximal and thin ice-distal varves do not accurately represent annual meltwater runoff and regional climate and thus were removed from the chronology. The sensitivity of varve couplet thickness to annual climate in New England, a region known to currently exhibit seasonal ENSO influence (20), makes the NE varve chronology a potentially ideal record for studying changes in ENSO or its teleconnections during the late Pleistocene. Perhaps more relevant than modern ENSO teleconnections in New England is evidence that the extratropical teleconnections of ENSO-related sea surface temperature patterns into this region were likely considerably stronger during glacial times (21). It is thus quite plausible that an analysis of the interannual temperature-related variability evident in this varve chronology might yield information regarding changes in ENSO or its teleconnections during the late Pleistocene.

In 1922, Antevs (18, 19) correlated >4000 varves within Glacial Lake Hitchcock and between contemporaneous glacial lakes in New England to create the original NE varve chronology. Antevs assembled this chronology by creating “normal” curves of average varve couplet thickness measurements from >100 correlated varve exposures. Multiple overlapping sections were measured to eliminate counting and measurement errors. The original NE varve chronology had two gaps within the series, which have now been corrected through paleomagnetic investigations in Vermont (22) and correlation from a core collected in Amherst, Massachusetts (23), yielding a continuous varve chronology (24).

The integrity of the NE varve chronology has been established through a variety of methods. First, many of the varve sections used by Antevs (18, 19) have been remeasured (22, 23); second, varve couplet thickness was measured in sections not used to formulate the original chronology (25); and third, paleomagnetic secular variation investigations (22, 25, 26) were performed to con-

¹Department of Geosciences, University of Massachusetts, Amherst, MA 01003, USA. ²Department of Environmental Sciences, University of Virginia, Charlottesville, VA 22903, USA.

*Present address: Department of Geosciences, University of Nebraska, Lincoln, NE 68588, USA.

†To whom correspondence should be addressed. E-mail: tammyr@unlserve.unl.edu

firm the correlation between overlapping segments. Most important, the previously floating chronology has now been fixed through careful accelerator mass spectrometry dating (22, 23, 25), confirming correlations within the chronology and providing well-constrained numerical dating of the NE varve chronology.

A number of regional varve thickness curves from the Glacial Lake Hitchcock portion of the NE varve chronology, deposited between 17,500 and 13,500 cal yr B.P., were combined to yield the continuous chronology analyzed here, NE varve numbers 2868 through 6900 [after correction for gaps in original chronology, see (22, 23)] (Fig. 2A). Before analysis, the raw varve chronologies were combined to yield a composite series representative of the underlying climate variability. Observations from modern lakes containing varved sediment indicate a logarithmic relation between varve thickness and early summer temperature, which influences meltwater and suspended sediment discharge (27, 28, and references therein). These underlying temperature variations, which typically exhibit a Gaussian distribution, are what we sought to isolate from the varve chronology. Consequently, a lognormal transformation of the varve thickness data was performed to yield a Gaussian-distributed time series appropriate for statistical analysis (Fig. 2B).

To facilitate joining the data sets into one continuous sequence, we removed low-frequency changes in varve thickness due to glacial retreat, readvances, and delta progradation by using a 200-year high-pass filter (Fig. 2C). This choice was relatively conservative; very low frequency climate variability was sacrificed to ensure that the residual higher frequency

variability was relatively free of nonclimatic influences. This trend removal is similar to that used to remove nonclimatic growth-related trends in dendroclimatic records (29). The data sets were subsequently normalized to have zero mean and unit standardization. This standardization procedure is similarly conservative, in that it will tend to remove long-term trends in climatic variance, rather than impose spurious trends, because the variance is equalized in distinct components of the chronology. Of primary interest here, however, is not the overall variance or the trend therein, but the distribution of variance with regard to time scale and how it changes over time. Finally, varve thicknesses in overlapping intervals were averaged to yield one continuous sequence of 4022 years (NE varve numbers 2868 through 6900). The high correlation between the overlapping segments (30) validated averaging the constituent segments to form one continuous chronology.

We analyzed the resulting transformed varve chronology for statistically significant narrowband or harmonic signals, using multiple-taper spectral analysis (31–35), and invoked the typical climatic null hypothesis of “red noise” (34, 35) (Fig. 3). An evolutive version of the spectral analysis (using a 600-year moving window) was performed to investigate the amplitude and frequency modulation of apparent signals in the record (Fig. 4). These analyses support the existence of significant narrowband signals, with time scales remarkably similar to those observed in the modern instrumental record (36, 37, and references therein) and Holocene paleoclimate records. In particular (see Fig. 3), statistically significant variability occurs at multidecadal (>40-year) time scales, at decadal-to-bidecadal (14-to-22-year) time scales, within the conventional 2.5-to-7-year band associated with ENSO, and at the 7-to-9-year period and ~2.1-year “quasi-biennial” period. The latter two time scales may be associated with the North Atlantic Oscillation (36, 38, 39, and references therein), although the 2.1-year-period signal should be interpreted cautiously because of its proximity to the 2-year Nyquist frequency for annual sampling. The 22-year-period signal has the same frequency as the Hale solar magnetic cycle, which has been argued to have a detectable influence in modern surface temperature records (40). Only about four peaks should exceed the 99% level on the basis of chance alone (41), suggesting that most of the >99% significant peaks in the spectrum are likely indicative of climate signals with preferred time scales.

Of particular interest are the highly significant spectral peaks (>99% level) between 2.5 and 5 years, within the conventional modern ENSO bandwidth (3 to 7 years), which are highly unlikely to have arisen from chance alone (41). The concentration of peaks in 4-to-5-, 3.3-to-3.5-, and 2.5-to-2.8-year bands within

the broader ENSO bandwidth is reminiscent of the modern ENSO spectral signature (36, and references therein). The 600-year window evolutive spectrum (Fig. 4) shows significant change in the 2.5-to-5-year ENSO band over time. To ensure that these changes are not an artifact of the statistical procedure used to combine overlapping varve segments, we performed spectral analyses of individual constituent segments. These analyses reproduced the original results. Similar frequency and amplitude modulation of the ENSO signal has been suggested to occur on multidecadal and century time scales in the recent past (4, 6–8) and can arise from natural variability in the coupled ocean-atmosphere system (42). The high-frequency (2.5-to-2.8-year peak) component is relatively robust and persistent throughout the varve record from 17,500 to 13,500 cal yr B.P. In contrast, the low-frequency (3.5-to-5-year) spectrum is strong from 17,500 to ~16,200 cal yr B.P., weakened from ~16,200 to ~15,200 cal yr B.P., and diminished to absent from ~15,200 to 13,500 cal yr B.P. This long-term trend of continual weakening of the interannual variability throughout the 4000-year record appears to be systematic rather than random in nature and may be associated with low-frequency astronomical forcing of ENSO (15, 16). The high-frequency (2.5-to-3-year) component of ENSO is typically associated with the lifetime of ENSO events and the El Niño/La Niña alteration, whereas the lower frequency (3-to-7-year) component is typically associated with the spacing of large events (43, 44). The absence of the lower frequency component of variability during the latter part of the interval studied here (i.e., the latest Pleistocene) is consistent with the theoretical prediction (15, 16) of fewer large events in the early Holocene.

Only the 15,000-year Ecuador debris-flow record of ENSO variability (13) overlaps in time with the NE varve chronology. These sediments show a similar trend of weakened ENSO-band variability from 15,000 to 7000 cal yr B.P. However, the lack of annual laminations in that record limits interpretations regarding true interannual ENSO variability. Rather, this record exhibits a dominant decadal (~15-year) time scale, which is typically associated with extratropical feedbacks (6, 45, 46) rather than the tropical dynamics governing interannual ENSO variability. Their observations in fact are consistent, for example, with the apparent pattern during the 17th through early 18th century, during which interannual variability in ENSO indices appears to have been largely suppressed, whereas decadal-scale variability nonetheless persisted (8).

Our results are consistent with model predictions using early Holocene insolation parameters (15). The coupled ocean-atmosphere model results for 11,000 cal yr B.P. (15) suggest a decreased amplitude of low-frequency (e.g., 4-to-7-year time scale) inter-

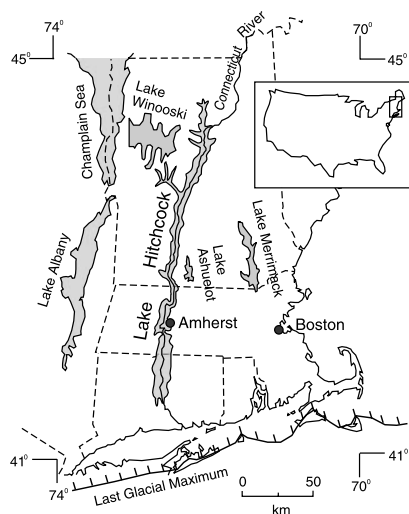


Fig. 1. Location of Glacial Lake Hitchcock in New England and nearby contemporaneous glacial lake systems from which the NE varve chronology was created.

REPORTS

annual variability but a persistence of high-frequency (e.g., 2-to-3-year range) ENSO variability. Lui *et al.* (15) suggested that this pattern of reduced low-frequency ENSO variability was caused by Asian monsoon intensification during increased insolation in the early Holocene. The gradual increase in solar insolation during the late Pleistocene may have caused the decreased low-frequency (3.3-to-5-year) ENSO variability seen in the NE varve chronology from ~15,500 to 13,500 cal yr B.P.

Despite the similarities between the ENSO pattern seen in the NE varve chronology and modern and paleoclimatic records, it is not possible to determine whether the changing intensity of the ENSO-like signal is directly related to El Niño intensity in the tropical Pacific Ocean. As discussed earlier [see (20, 21)], one would expect ENSO to influence seasonal melt patterns in New England during the late Pleistocene. However, ENSO teleconnections into New England may have been continually altered as boundary conditions changed during ice retreat. It is plausible that the retreat of the Laurentide ice margin, with its tendency to

deflect extratropical storm tracks, could have led to a slow northward migration of storm tracks and thus ENSO teleconnections into North America, which represent a modulation of these storm track patterns. However, varve deposition in Glacial Lake Hitchcock followed the ice margin with progressively younger

varves deposited northward, therefore limiting this effect. Although the persistent high-frequency component of the ENSO band throughout the NE varve chronology argues against any dominant influence of nonstationary teleconnections, the possibility nonetheless remains that the observed changes are influ-

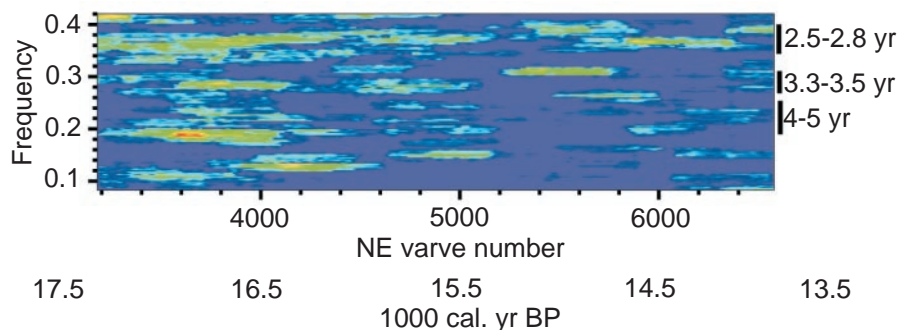


Fig. 4. Evolutive spectral analysis from the NE varve chronology data set (NE varve numbers 2868 through 6900) covering the interval from 17,500 to 13,500 cal yr B.P. The spectrum is normalized everywhere by the median red noise level, so that the amplitude shown is proportional to the associated level of statistical significance. The background color is set to the median red noise level (50% confidence), and features evident above the background are significant at the >50% confidence level, with the lightest features being the most significant.

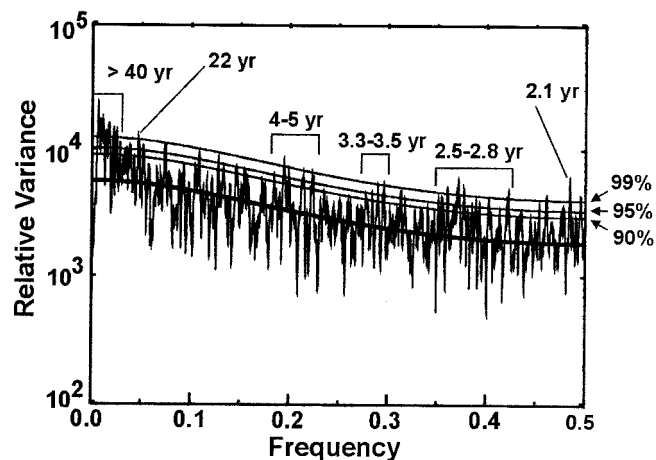
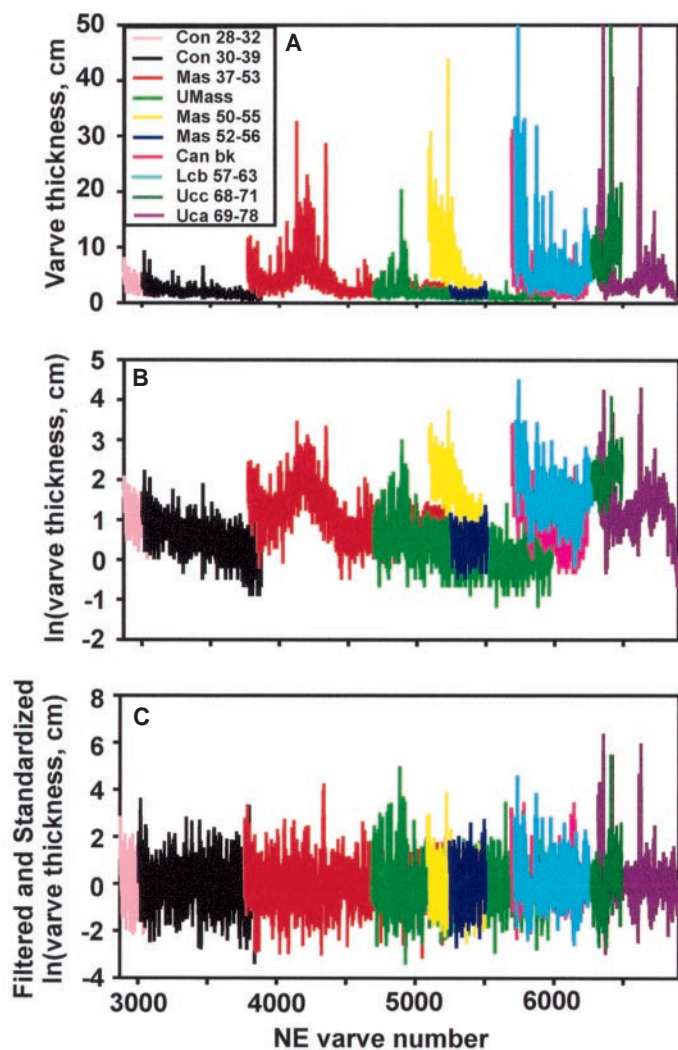


Fig. 2 (left). Normal curve varve thickness data sets from the Glacial Lake Hitchcock portion of the NE varve chronology used for spectral analysis (NE varves 2868 through 6900, 17,500 through 13,500 cal yr B.P.) (data sets used are available at www.sciencemag.org/feature/data/1047305.shl). (A) Original raw varve couplet thickness measurements, (B) natural log of varve thickness data, and (C) data after standardization (zero mean and unit standard deviation) and high-pass filtering (removal of time scales of 200-year and longer periods) are given. **Fig. 2 (right).** Multitaper method spectral analysis (31, 33) of NE varve chronology data set (NE varve numbers 2868 through 6900) covering the interval from 17,500 to 13,500 cal yr B.P. The median red noise level is shown by the thick curve, and 90, 95, and 99% confidence levels relative to red noise are shown by the thin curves. Significant spectral peaks are labeled.

enced by some combination of changes in the nature of ENSO teleconnections into North America and changes in ENSO itself. Our primary conclusion, that ENSO was active during the late Pleistocene, follows, however, in either scenario.

References and Notes

1. K. E. Trenberth and T. J. Hoar, *Geophys. Res. Lett.* **24**, 3057 (1997).
2. T. R. Knutson, S. Manabe, D. Gu, *J. Clim.* **10**, 138 (1997).
3. L. Goddard and N. E. Graham, *J. Geophys. Res.* **102**, 10423 (1997).
4. B. Wang and Y. Wang, *J. Clim.* **9**, 1586 (1996).
5. J. Cole and E. Cook, *Geophys. Res. Lett.* **25**, 4529, (1998).
6. M. E. Mann, R. S. Bradley, M. K. Hughes, in *El Niño and the Southern Oscillation: Multiscale Variability and Its Impacts on Natural Ecosystems and Society*, H. F. Diaz and V. Markgraff, Eds. (Cambridge Univ. Press, Cambridge, in press).
7. D. W. Stahle et al., *Bull. Am. Meteorol. Soc.* **79**, 2137 (1998).
8. R. B. Dunbar, G. M. Wellington, M. W. Colgan, P. W. Glynn, *Paleoceanography* **9**, 291 (1994).
9. M. K. Gagan et al., *Science* **279**, 1014 (1998).
10. J. Shulmeister and B. G. Lees, *Holocene* **5**, 10 (1995).
11. D. H. Sandweiss, J. B. Richardson III, E. J. Reitz, H. B. Rollins, K. A. Maasch, *Science* **273**, 1531 (1996).
12. T. J. DeVries, L. Ortlieb, A. Diaz, L. Wells, Cl. Hillaire-Marcel, *Science* **276**, 965 (1997).
13. D. T. Rodbell et al., *Science* **283**, 516 (1999).
14. H. S. Godsey, T. C. Moore Jr., D. K. Rea, L. C. K. Shane, *Can. J. Earth Sci.* **36**, 533 (1999).
15. Z. Lui, R. Jacob, J. Kutzbach, S. Harrison, J. Anderson, *PAGES Newsletter* **7** (no. 2), 16 (1999).
16. A. C. Clement, R. Seager, M. A. Cane, *Paleoceanography* **14**, 441 (1999).
17. G. M. Ashley, in *Glaciofluvial and Glaciolacustrine Sedimentation*, A. V. Jopling and C. McDonald, Eds. (Society of Economic Paleontologists and Mineralogists, Tulsa, OK, 1975), pp. 304–320.
18. E. Antevs, *Am. Geogr. Soc. Res. Ser.* **11**, 1 (1922).
19. _____, *Am. Geogr. Soc. Res. Ser.* **17**, 1 (1928).
20. M. S. Halpert and C. F. Ropelewski, *J. Clim.* **5**, 577 (1992).
21. J. H. Yin and D. S. Battisti, *J. Clim.*, in press.
22. J. C. Ridge et al., *Geogr. Phys. Quat.* **53**, 1 (1999).
23. T. M. Rittenour, thesis, University of Massachusetts, Amherst (1999).
24. The Claremont gap in the NE varve chronology separated varves from the lower (NE varves 2701 through 6352) and upper (NE varves 6601 through 7750) Connecticut River valley (Glacial Lake Hitchcock). Ridge et al. (22) linked the two sequences (lower NE varve 6012 = upper NE varve 6601) to correct this gap. The Hudson Valley gap (NE varves 5600 through 5709) consisted of varves from Lake Albany that were used to span an interval not covered in Glacial Lake Hitchcock. Correlation with a core from Glacial Lake Hitchcock (23) has indicated a 10-varve error in the sequence (NE varves 5669 through 5678), which has been removed from the NE varve chronology (varve numbers were not adjusted, numbers 5669 through 5678 were just removed from the chronology).
25. J. C. Ridge and F. D. Larsen, *Geol. Soc. Am. Bull.* **102**, 889 (1990).
26. K. L. Verosub, *Geophys. Res. Lett.* **6**, 245 (1979).
27. K. Hughen, J. T. Overpeck, R. Anderson, *Holocene* **10**, 9 (2000).
28. D. R. Hardy, B. S. Bradley, B. Zolitschka, *J. Paleolimnol.* **16**, 227 (1996).
29. E. R. Cook, K. R. Briffa, D. M. Meko, D. A. Graybill, G. Funkhouser, *Holocene* **5**, 229 (1995).
30. Correlation between these data sets was highly statistically significant [correlation coefficients ranged from $r = 0.9$ to 0.4 for 100 or more overlapping samples]. In one overlapping segment with only eight points in common, a statistically meaningful correlation was not obtained.
31. D. J. Thomson, *Proc. IEEE* **70**, 1055 (1982).

32. J. Park, C. R. Lindberg, F. L. Vernon III, *J. Geophys. Res.* **92**, 12675 (1987).
33. We used the multitaper method of spectral analysis (31, 32) based on $p = 8$ tapers and a time-frequency half-bandwidth product of $W = 5N$ as a compromise between spectral bandwidth and the stability of the spectrum estimate. The 4022 independent annual values were zero-padded to the nearest power of 2 ($N = 4096$), providing $2048/5 = 410$ approximately independent estimates of the amplitude of the spectrum.
34. M. E. Mann and J. Lees, *Clim. Change* **33**, 409 (1996).
35. Significance of narrowband features in the spectrum relative to the null hypothesis of red noise was determined with the robust method of noise background estimation of Mann and Lees (34). This analysis incorporates a separate application of Thomson's (31) F -test criterion for phase coherence to determine if the underlying signal is simply a narrowband feature of the spectrum or if it is a true harmonic oscillatory signal.
36. M. E. Mann and J. Park, *J. Geophys. Res.* **99**, 25819 (1994).
37. M. Ghil and R. Vautard, *Nature* **350**, 324 (1991).
38. J. W. Hurrell, *Geophys. Res. Lett.* **23**, 665 (1996).
39. E. R. Cook, R. D. D'Arrigo, K. R. Briffa, *Holocene* **8**, 9 (1998).
40. T. Baranyi, A. Ludmany, H. Coffey, *Geophys. Res. Lett.* **25**, 2269 (1998).
41. Given the time-frequency bandwidth of the analysis (31), one would expect 1% of 410, or ~ 4 , spurious

peaks at the 99% level, arising from random statistical fluctuations alone, including only 2 in the frequency range of 0.2 to 0.4 cycles per year.

42. S. E. Zebiak and M. A. Cane, in *Greenhouse-Gas-Induced Climate Change: A Critical Appraisal of Simulations and Observations*, M. E. Schlesinger, Ed. (Elsevier, New York, 1991), pp. 457–469.
43. N. E. Graham and W. B. White, *Science* **240**, 1293 (1988).
44. S. E. Zebiak and M. A. Cane, *Mon. Weather Rev.* **115**, 2262 (1987).
45. K. E. Trenberth, *Bull. Am. Meteorol. Soc.* **71**, 988 (1990).
46. Y. Zhang, J. M. Wallace, D. S. Battisti, *J. Clim.* **10**, 1004 (1997).
47. The authors thank J. Ridge, Tufts University, for providing varve thickness measurements from the NE varve chronology and his own measured sections, along with providing useful information regarding the dating of the varve chronology. T.M.R. acknowledges support from the Geological Society of America, Sigma Xi, and the Department of Geosciences at the University of Massachusetts. J.B.-G. acknowledges support from National Geographic and a University of Massachusetts faculty grant. M.E.M. acknowledges support from NOAA and NSF through the Earth Systems History Program and from the U.S. Department of Energy through the Alexander Hollaender Distinguished Postdoctoral Fellowship Program.

22 November 1999; accepted 24 March 2000

Reduction of Tropical Cloudiness by Soot

A. S. Ackerman,^{1*} O. B. Toon,² D. E. Stevens,³ A. J. Heymsfield,⁴ V. Ramanathan,⁵ E. J. Welton⁶

Measurements and models show that enhanced aerosol concentrations can augment cloud albedo not only by increasing total droplet cross-sectional area, but also by reducing precipitation and thereby increasing cloud water content and cloud coverage. Aerosol pollution is expected to exert a net cooling influence on the global climate through these conventional mechanisms. Here, we demonstrate an opposite mechanism through which aerosols can reduce cloud cover and thus significantly offset aerosol-induced radiative cooling at the top of the atmosphere on a regional scale. In model simulations, the daytime clearing of trade cumulus is hastened and intensified by solar heating in dark haze (as found over much of the northern Indian Ocean during the northeast monsoon).

A primary objective of the Indian Ocean Experiment (INDOEX) was to quantify the indirect effect of aerosols on climate through their effects on clouds (1). Conventionally, increased aerosol concentrations are expected to increase cloud droplet concentrations, and hence, total droplet cross-sectional area, thereby causing more sunlight to be reflected to space (2). Furthermore, model simulations

of marine stratocumulus (3–5) and observations of ship tracks (6–8) suggest that increased aerosol concentrations can enhance cloud water content, physical thickness, and areal coverage by decreasing precipitation. Deep layers of dark (solar-absorbing) haze were observed over much of the tropical northern Indian Ocean in February–March of 1998 and 1999 during INDOEX (9, 10). The clouds observed in the Northern Hemisphere were typically embedded in the haze (Fig. 1). In contrast to the conventional expectation that aerosols augment cloud depth and coverage, very sparse cloud cover is found in that region during that time of year (11). These INDOEX observations suggest a new mechanism by which aerosols impact clouds, in which a dark haze can significantly reduce areal coverage of trade cumulus (the predom-

¹NASA Ames Research Center, Moffett Field, CA 94035, USA. ²University of Colorado, Boulder, CO 80309, USA. ³Lawrence Livermore National Laboratory, Livermore, CA 94551, USA. ⁴National Center for Atmospheric Research, Boulder, CO 80301, USA. ⁵Scripps Institution of Oceanography, La Jolla, CA 92093, USA. ⁶Science Systems and Applications, Greenbelt, MD 20771, USA.

*To whom correspondence should be addressed. E-mail: ack@sky.arc.nasa.gov